Journal of Magnetic Resonance 309 (2019) 106617

Contents lists available at ScienceDirect

Journal of Magnetic Resonance

journal homepage: www.elsevier.com/locate/jmr

First hyperpolarized [2-^{13}C]pyruvate MR studies of human brain metabolism

Brian T. Chung [a,b,*], Hsin-Yu Chen [a], Jeremy Gordon [a], Daniele Mammoli [a], Renuka Sriram [a], Adam W. Autry [a], Lydia M. Le Page [a,c], Myriam M. Chaumeil [a,c], Peter Shin [a], James Slater [a], Chou T. Tan [d], Chris Suszczynski [d], Susan Chang [e], Yan Li [a], Robert A. Bok [a], Sabrina M. Ronen [a], Peder E.Z. Larson [a], John Kurhanewicz [a], Daniel B. Vigneron [a]

[a] Department of Radiology and Biomedical Imaging, University of California, San Francisco, CA 94158, USA
[b] UCSF – UC Berkeley Graduate Program in Bioengineering, University of California, USA
[c] Department of Physical Therapy and Rehabilitation Science, University of California, San Francisco, CA 94158, USA
[d] ISOTEC Stable Isotope Division, MilliporeSigma, Merck KGaA, Miamisburg, OH 45342, USA
[e] Department of Medicine, University of California, San Francisco, CA 94158, USA

ARTICLE INFO

Article history:
Received 16 July 2019
Revised 4 October 2019
Accepted 6 October 2019
Available online 8 October 2019

Keywords:
Hyperpolarized C13
Metabolic imaging
Brain metabolism

ABSTRACT

We developed methods for the preparation of hyperpolarized (HP) sterile [2-^{13}C]pyruvate to test its feasibility in first-ever human NMR studies following FDA-IND & IRB approval. Spectral results using this MR stable-isotope imaging approach demonstrated the feasibility of investigating human cerebral energy metabolism by measuring the dynamic conversion of HP [2-^{13}C]pyruvate to [2-^{13}C]lactate and [5-^{13}C]glutamate in the brain of four healthy volunteers. Metabolite kinetics, signal-to-noise (SNR) and area-under-curve (AUC) ratios, and calculated [2-^{13}C]pyruvate to [2-^{13}C]lactate conversion rates (k_{PL}) were measured and showed similar but not identical inter-subject values. The k_{PL} measurements were equivalent with prior human HP [1-^{13}C]pyruvate measurements.

1. Introduction

Dissolution Dynamic Nuclear Polarization (dDNP) provides over 10,000 fold signal enhancement for hyperpolarized carbon-13 (HP-^{13}C) MRI, enabling a novel stable-isotope molecular imaging approach for preclinical and recently clinical research studies demonstrating both safety and translational potential for human HP-^{13}C molecular imaging [1–4]. HP [1-^{13}C]pyruvate MR metabolic imaging has been applied to identify tumor metabolism [5], assess aggressiveness [6], evaluate treatment response [7], and probe organ function [4,8].

MR detection of the conversion of HP [1-^{13}C]pyruvate to [1-^{13}C]lactate catalyzed by lactate dehydrogenase (LDH) has shown research value and clinical potential in Phase I trials of cancer patients reflecting the Warburg Effect [3] with greatly upregulated LDH activity [9,10]. In approaching the tricarboxylic acid (TCA) cycle, [1-^{13}C]pyruvate is enzymatically metabolized via pyruvate dehydrogenase (PDH) and converted to $^{13}CO_2$, thereby preventing direct detection of downstream TCA cycle metabolites. Prior animal studies using HP pyruvate with the ^{13}C isotope enriched in the 2-position ([2-^{13}C]pyruvate) have successfully shown direct detection as the HP ^{13}C labeled atoms are carried over into acetyl-CoA, a precursor to the TCA cycle, and on to [5-^{13}C]glutamate, acetyl-carnitine and other metabolites as shown in Fig. 1 [11,12]. Therefore, HP [2-^{13}C]pyruvate provides novel metabolic information different from HP [1-^{13}C]pyruvate due to its unique positioning atop multiple anaplerotic and cataplerotic metabolic cascades in the TCA cycle with known fast conversions [13]. Prior preclinical studies have shown differences in [2-^{13}C]pyruvate to [5-^{13}C]glutamate metabolism with isocitrate dehydrogenase (IDH) mutations in brain tumor models that are not detected by HP [1-^{13}C]pyruvate MR [14].

The goal of this study was to develop methods for the hyperpolarization and preparation of sterile [2-^{13}C]pyruvate with FDA-IND and IRB approval for first-ever human studies. We sought to investigate HP [2-^{13}C]pyruvate conversion to [2-^{13}C]lactate and [5-^{13}C]glutamate in the normal brain in four volunteers, demonstrating a significant first step for HP metabolic imaging to diagnose neurological disorders potentially at an early stage and monitor

* Corresponding author at: Department of Radiology and Biomedical Imaging, University of California, San Francisco, 1700 Fourth Street, Byers Hall Suite 102, San Francisco, CA 94158, USA.
E-mail address: Brian.Chung@ucsf.edu (B.T. Chung).

https://doi.org/10.1016/j.jmr.2019.106617
1090-7807/

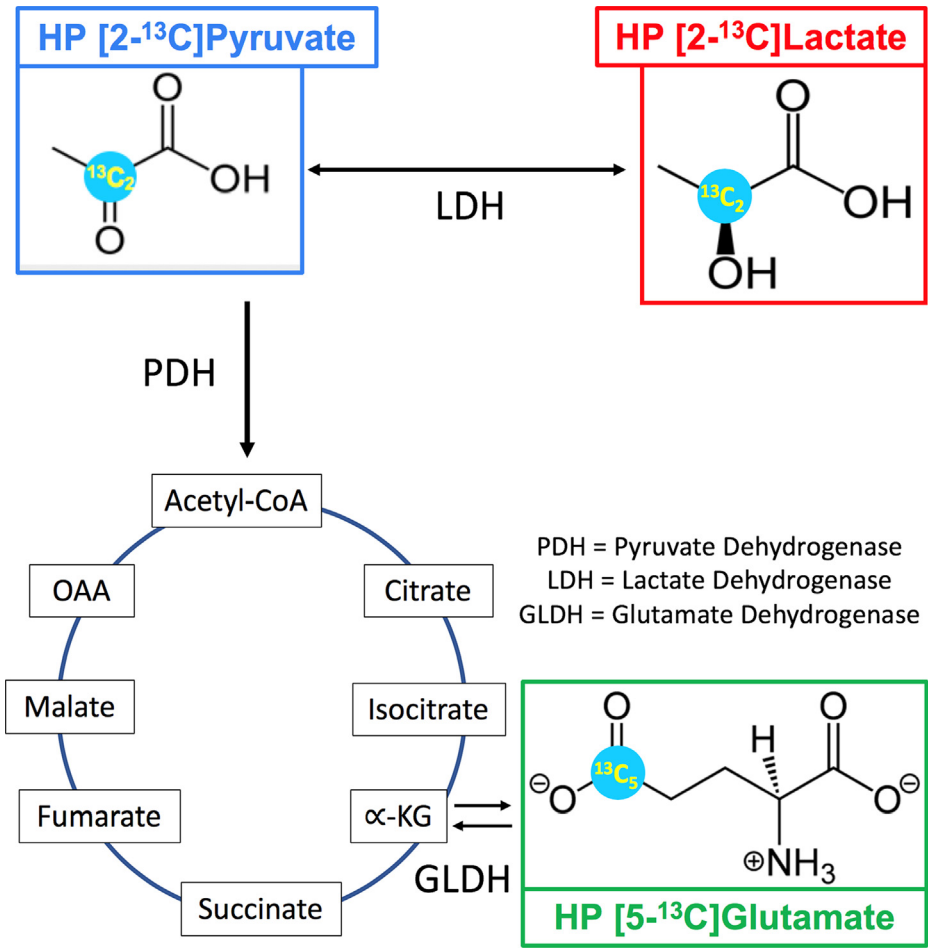

Fig. 1. Diagram showing [2-^{13}C]pyruvate metabolism investigated in this hyperpolarized NMR spectroscopy study of the human brain.

treatment response. Unlike animal studies, these human experiments were performed without anesthesia that significantly reduces brain pyruvate metabolism [15] and therefore are more relevant to future patient studies.

2. Methods

2.1. [2-^{13}C]Pyruvate: FDA-IND, IRB, human volunteers

[2-^{13}C]pyruvate was produced by MilliporeSigma Isotec Stable Isotopes (Miamisburg, OH) following Good Manufacturing Practices (GMP) for first-ever use in human HP MR studies. All human studies followed an IRB and FDA IND-approved protocol with informed consent. Proton T2-FLAIR anatomical reference imaging scans showed volunteers had no acute abnormalities.

2.2. Preclinical quality control: T1, polarization, purity, animal studies

T1 relaxation times and liquid-state polarization levels of [2-^{13}C]pyruvate were measured with independent characterization experiments in solution and murine models. [2-^{13}C]pyruvate T1 measurements of 47 sec and polarization levels of 15.61% reaffirmed literature values [16]. Pyruvic acid solution NMR testing was performed using a Varian VNMRS 500 MHz (Varian Medical Systems, Palo Alto, CA) to confirm the absence of impurities.

In-vivo spectroscopic animal studies were performed on a 3 T GE MR scanner following IACUC approval, prior to human volunteer studies to test *in vivo* performance. Non-localized dynamic ^{13}C NMR spectra were acquired with hard-pulsed excitation (TR/TE = 3 sec/35 msec) in Sprague-Dawley rats for detection of [5-^{13}C]glutamate, [2-^{13}C]lactate and other metabolite resonances such as acetylcarnitine and acetoacetate [17].

2.3. Clinical preparation: SPINlab hyperpolarization

A 1.46 g sample of 14 M 99% enriched [2-^{13}C]-labeled pyruvic acid (Millipore-Sigma, Miamisburg, OH) mixed with 15 mM trityl radical (GE Healthcare, Oslo, Norway) was pre-filled in a single-use, pharma-kit polymer fluid pathway and polarized for over 2 h in a SPINlab polarizer (General Electric, Niskayuna, NY) operating at 5 Tesla and 0.77 Kelvin, with microwave irradiation frequency in the 94.0–94.1 GHz band. Following the protocol approved by the University of California San Francisco IRB and the FDA IND, and after dissolution and meeting all quality control specifications and pharmacist approval, 0.43 mL/kg of the hyperpolarized pyruvate solution (250 mM) was injected intravenously at a rate of 5 mL/sec using a power injector (Medrad Inc., Warrendale, PA) followed by 20 mL of sterile saline.

2.4. MR protocol

Volunteers were measured using a 3 T MR scanner (MR750, 50 mT/m gradient amplitude, 200 T/m/sec slew rate; GE Healthcare, Waukesha, WI) and scanned with a volume excitation and 32-channel receive ^{13}C array coil for brain studies [18]. A 400 μsec hard pulse excitation provided an approximately 2.5 kHz

excitation bandwidth, with a nominal flip angle of 40° at the center frequency of 141 ppm calibrated using a built-in urea phantom. The [2-^{13}C]pyruvate, [5-^{13}C]glutamate, and [2-^{13}C]lactate doublet resonances were excited with 7°, 30°, 5° and 2.1° flip angles respectively. The acquisition used temporal and spectral resolutions of 2 sec and 2.4 Hz across 30 timepoints for a total scan time of 2 min.

2.5. Data analysis

Dynamic spectroscopic data yielding kinetic rates and curves was reconstructed after zero-filling free induction decays. The 32-channel data was combined with a phase-sensitive summation followed by line broadening of 5 Hz [19].

For the pyruvate-to-lactate conversion (k_{PL}) kinetic model, the measured pyruvate magnetization functioned as the input for fitting the lactate magnetization. The MATLAB model was solved based on minimization of a constrained least-squares error computed across measured and estimated lactate using a trust-region-reflective algorithm. The input-less fitting was chosen over integral ratios due to improved accuracy by accounting for variability in delivery times [20]. The analytical tools used are available from the Hyperpolarized MRI Toolbox via the Hyperpolarized Technology Resource Center: https://doi.org/10.5281/zenodo.1198915.

Quantitative data processing and display were performed using MATLAB (The MathWorks Inc., Natick, MA) and MestReNova (Mestrelab, Santiago de Compostela, Spain). Zero- and first-order phase corrections were performed, and baseline was subtracted by fitting a spline to signal-free regions of the smoothed spectrum. Metabolites of interest were quantified following prior assignments by selecting and integrating across peak boundaries [17]. Single timepoint data 16 sec following injection was further analyzed and interpreted after performing singular value decomposition (SVD) signal enhancement techniques [20–22,24].

3. Results

3.1. Volunteer spectra

HP [2-^{13}C]pyruvate, [2-^{13}C]lactate, [5-^{13}C]glutamate and other metabolites were successfully observed and quantitatively measured for the first time in four volunteers. Fig. 2 shows a representative summed spectra over the total 2 min scan time for a healthy volunteer using a pulse and acquire scheme with the RF profile shown in Fig. 3. Figs. 4 and 5 depict spectra and kinetics of measured metabolite resonances for each of the four volunteers.

3.2. SNR & metabolite ratios

Tables 1 and 2 summarize measured SNR from the single timepoint data and AUC metabolite ratios summed across all timepoints for 4 volunteers. Measured values and calculated mean and standard error across volunteers were consistent within expected ranges [16]. The observed variations in SNR can be attributed to multiple factors including brain volumes, polarization values, and delivery times from the polarizer to the subject. These demonstrated however minimal effects on the ratios and kinetic values that showed tight agreement between volunteers. The third volunteer dataset showed the highest SNR with AUC ratios near median and was hence selected as the representative spectrum for peak identification in Fig. 2. The [2-^{13}C]lactate (left and right peaks) correspond to the left and right resonances of the [2-^{13}C] lactate doublet in the ^{13}C MRS spectra. The left (downfield)

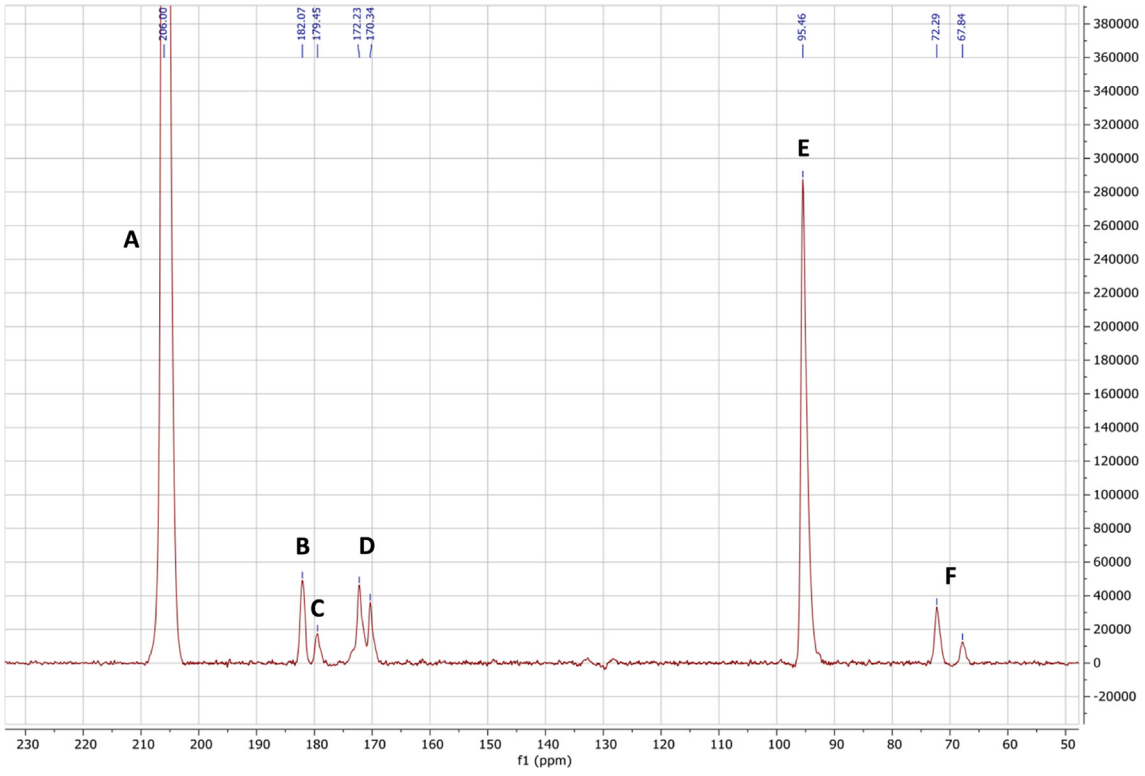

Fig. 2. Representative Carbon-13 NMR summed spectrum from the brain of a healthy volunteer acquired with a 32-channel head coil following an injection of 1.43 mL/kg of 250 mM [2-^{13}C]pyruvate. Peak identification was assigned following those by Park et al. from studies of HP [2-^{13}C]pyruvate in the murine brain: (A) [2-^{13}C]pyruvate, (B) [5-^{13}C]glutamate, (C) [1-^{13}C]citrate and/or [5-^{13}C]glutamine, (D) [1-^{13}C]pyruvate (natural abundance doublet), (E) [2-^{13}C]pyruvate-hydrate, (F) [2-^{13}C]lactate doublet [17].

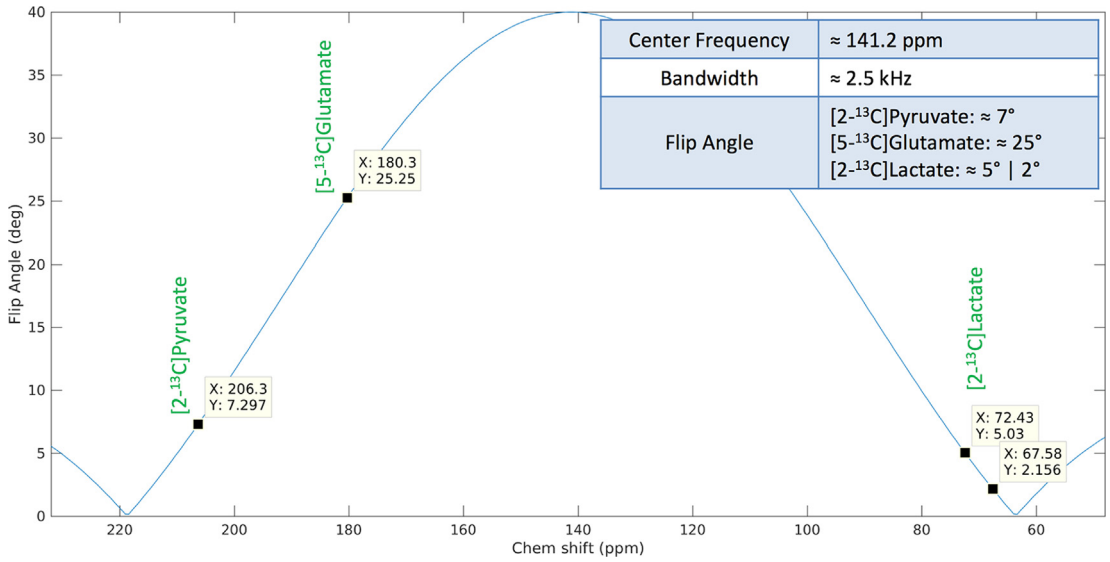

Fig. 3. Flip angle plot of the RF excitation pulse sequence with the parameters used for this study. Note the decreased excitation of the upfield [2-^{13}C]lactate resonance versus the downfield by approximately one half.

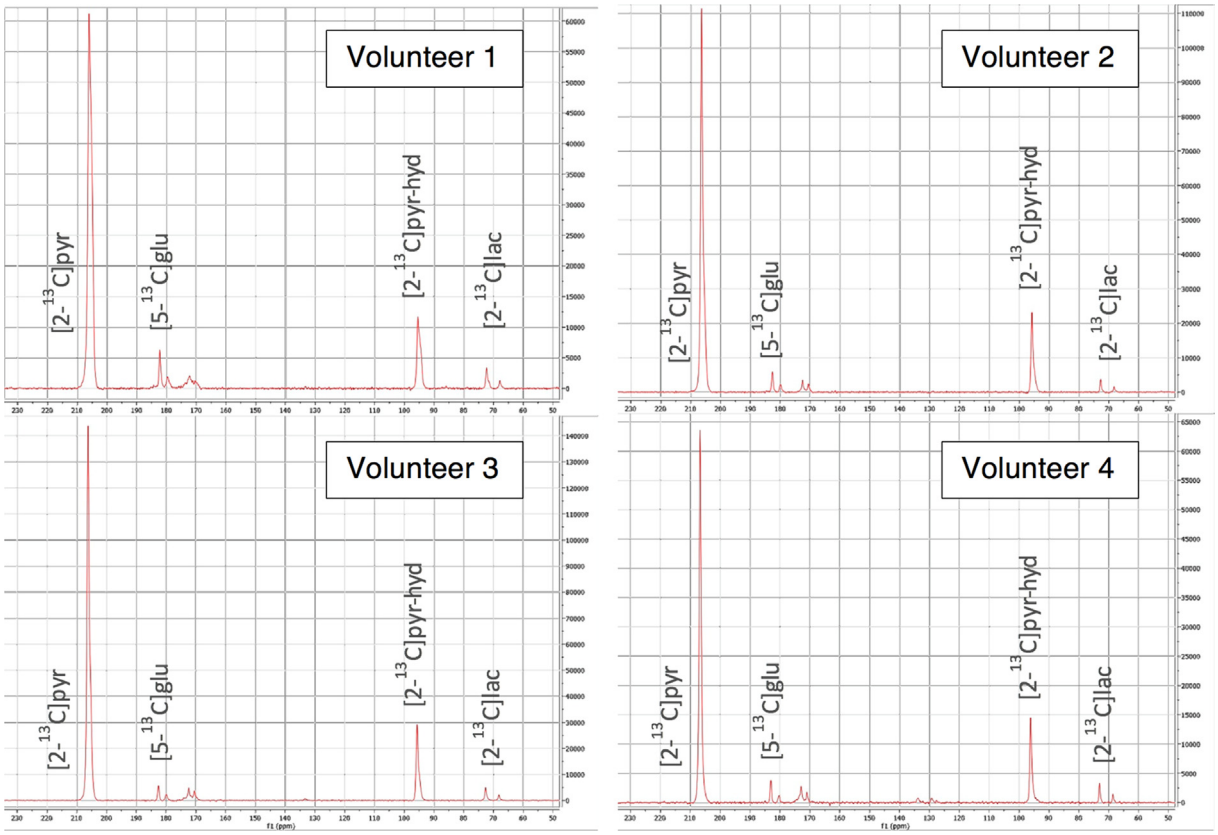

Fig. 4. Spectra for all four volunteers at a single timepoint 16 sec post-injection. Similar levels of [5-^{13}C]glutamate and [2-^{13}C]lactate reflect the underlying biochemistry of the healthy human brain of similar rates of conversion of [2-^{13}C]pyruvate to [2-^{13}C]lactate catalyzed by LDH as [2-^{13}C]pyruvate to [5-^{13}C]glutamate catalyzed by PDH.

resonance is about two-fold higher due to the excitation profile shown in Fig. 3.

3.3. [2-^{13}C]Pyruvate k_{PL} Model:

Fig. 6 shows a MATLAB plot of a measured [2-^{13}C]pyruvate k_{PL} value from the volunteer studies with calculated mean and standard error of 0.011 ± 0.002 sec^{-1}. The values were consistent with prior [1-^{13}C]pyruvate k_{PL} values of 0.012 sec^{-1} acquired using a similar setup and non-selective pulse-acquire strategy [17,20]. Identical results of pyruvate to lactate kinetics across a previously processed [1-^{13}C]pyruvate dataset and newly acquired [2-^{13}C] pyruvate datasets from volunteers lends verification to the robustness and consistency of approach.

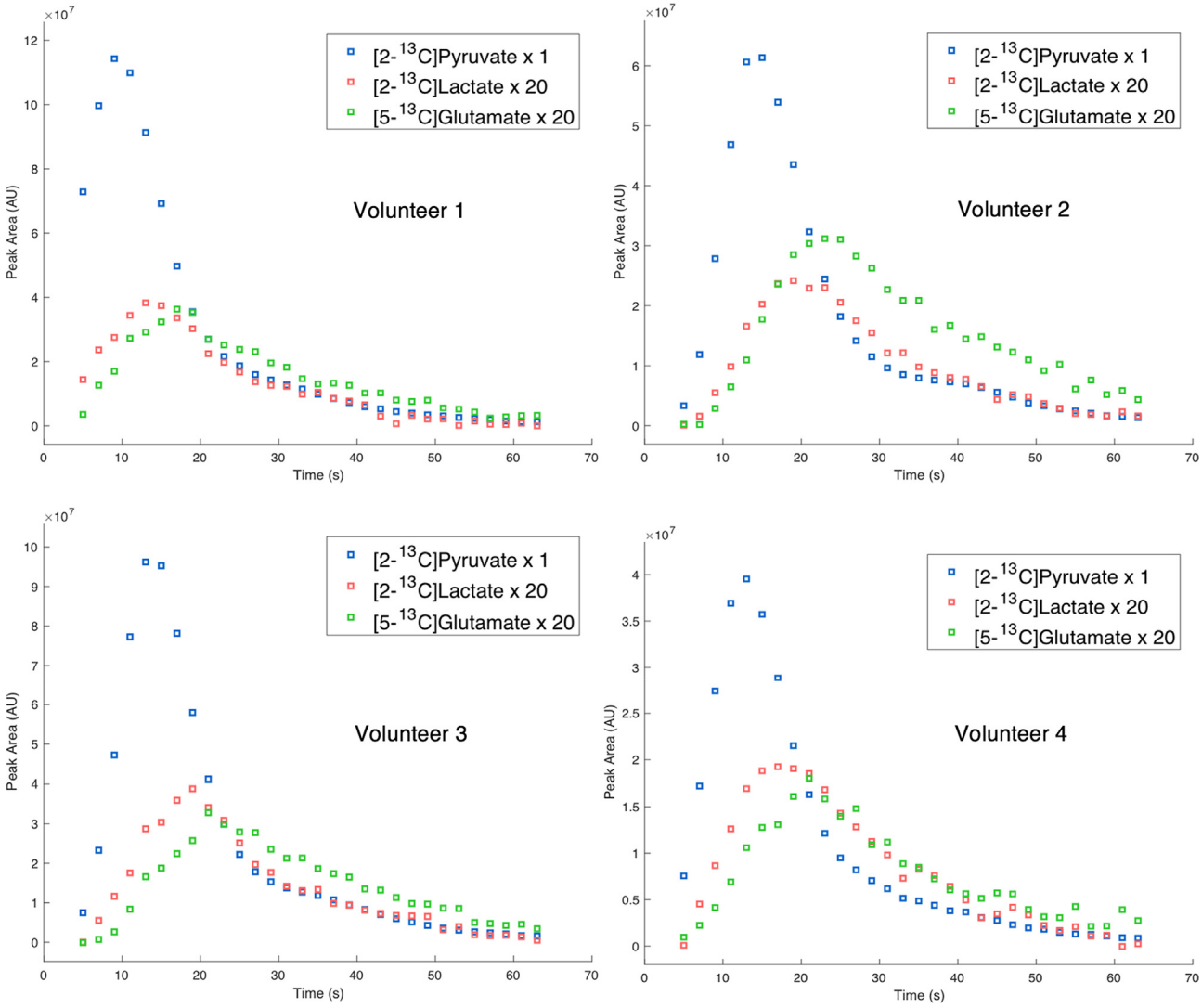

Fig. 5. Dynamic plots of metabolite kinetics for each of the four volunteers. Results were consistent noting minor differences in intensity scale. As shown in the corresponding Fig. 4, the rates of conversion of [2-^{13}C]pyruvate to [2-^{13}C]lactate and [5-^{13}C]glutamate are similar in the normal human brain.

Table 1
SNR for each volunteer from a single timepoint 16 sec post-injection with calculated mean and standard error.

Volunteer	[2-^{13}C]Pyruvate	[5-^{13}C]Glutamate	[2-^{13}C]Pyruvate-Hydrate	[2-^{13}C]Lactate (Left Peak)	[2-^{13}C]Lactate (Right Peak)
1	885.93	91.18	169.68	24.63	9.55
2	1278.34	68.36	265.33	42.58	18.55
3	2114.06	83.03	428.07	72.67	32.95
4	964.09	57.43	219.63	50.93	22.05
Mean	1310.61 ± 486.57	75.00 ± 13.03	270.68 ± 96.96	47.70 ± 17.27	20.77 ± 8.38

Table 2
AUC metabolite ratios for each volunteer summed across all timepoints with calculated mean and standard error.

Volunteer	Lac/Pyr	Glu/Pyr	Pyr-Hyd/Pyr	Glu/Lac
1	0.024	0.027	0.163	1.125
2	0.030	0.045	0.178	1.500
3	0.028	0.030	0.180	1.071
4	0.038	0.037	0.191	0.974
Mean	0.030 ± 0.005	0.035 ± 0.007	0.178 ± 0.010	1.168 ± 0.199

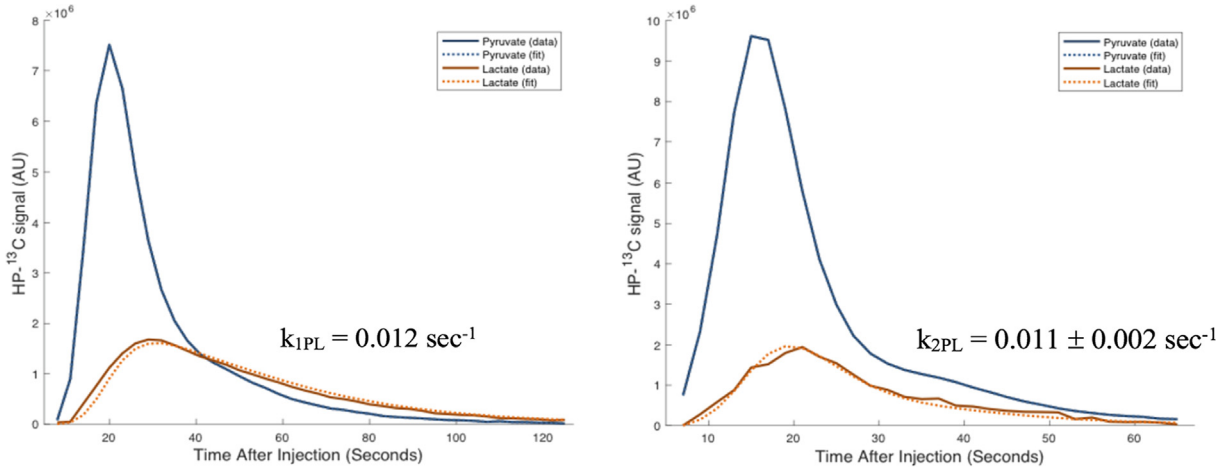

Fig. 6. Plots showing k_{PL} analysis demonstrated similar results between a previously acquired [1-^{13}C]pyruvate dataset from a volunteer (left) and [2-^{13}C]pyruvate volunteer dataset acquired in this study with the mean ± standard error for all 4 volunteers (right).

3.4. Initial volunteer EPI studies

Fig. 7 shows initial data and feasibility of HP ^{13}C imaging of the [2-^{13}C]pyrvuate conversion to [5-^{13}C]glutamate using a specialized ^{13}C 32-channel head coil. As shown in Fig. 2 not only was the uptake of HP [2-^{13}C]pyruvate in the human brain observed, but also its metabolic conversion to [2-^{13}C]lactate, [5-^{13}C]glutamate, and other metabolites, similar to prior animal study results [17].

4. Discussion and conclusion

In this study we worked with the ISOTEC Stable Isotope Division of MilliporeSigma, Merck KGaA to develop GMP grade 99% enriched [2-^{13}C]pyruvate meeting the purity specifications established for [1-^{13}C]pyruvate used in numerous human studies following FDA-IND and IRB approved protocols. Prior to human studies with HP [2-^{13}C]pyruvate, we first tested the purity and polarization through *in vitro* NMR analysis and performed a process qualification for testing and demonstrating the sterility of the polarized solution. The NMR spectra in Fig. 4 and quantitative values in Tables 1 and 2 demonstrated excellent data repeatability affirming the consistency of the preparation and processing methods. Metabolite ratios and dynamic plots in these initial studies directly reflected the excitation profile of the RF pulse that was optimized to capture the bandwidth encompassing metabolic byproducts and provided normative values for future human brain HP [2-^{13}C]pyruvate NMR studies. Lastly pyruvate to lactate kinetic

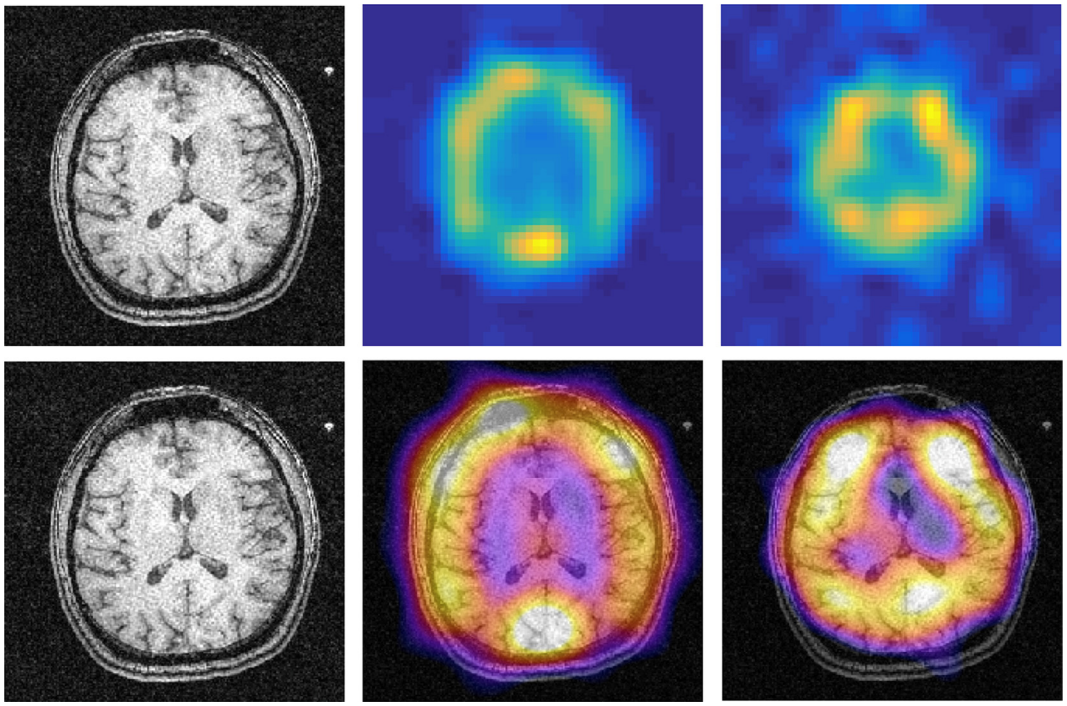

Fig. 7. Images acquired using a metabolite-specific flip angle schedule and echo planar imaging (EPI) readout. From left to right ^{1}H proton reference image, overlaid [2-^{13}C] pyruvate, and [5-^{13}C]glutamate images of a volunteer's brain are shown. The single-shot HP ^{13}C EPI images were acquired with: in-plane resolution = 2.5 × 2.5 cm^2, slice thickness = 5 cm, bandwidth = 8.06 kHz, TR = 100 msec, temporal resolution = 3 sec, TE = 19 msec, and flip angles θ_{Pyr} = 10°, θ_{Glu} = 60°. Average SNR of the pyruvate signal = 682 and glutamate signal = 31.1.

modeling from these [2-^{13}C]pyruvate studies yielded k_{PL} values that were consistent with results from a prior HP [1-^{13}C]pyruvate dataset in healthy human brain.

4.1. Future directions

This study demonstrated feasibility and initial normative values for HP [2-^{13}C]pyruvate NMR and thus serves as the groundwork for designing new studies of neurological disorders. These future studies would clearly benefit from an imaging approach to investigate HP [2-^{13}C]pyruvate MRI variations associated with anatomy and pathology and examine differences using centrality metrics and connectomic analytical methods with HP [1-^{13}C]pyruvate MRI [22]. HP metabolic information can also be linked with modalities such as functional and diffusion MRI to build increasingly comprehensive representations of neural function, structure and metabolism [23]. Centrality metrics processing higher-order descriptors of multi-valued metabolite kinetics with advances in machine learning may further elucidate new methods for detecting early stages of neurological disorders.

Declaration of Competing Interest

The authors declare that they have no known competing financial interests or personal relationships that could have appeared to influence the work reported in this paper.

Acknowledgements

This work was supported by NIH grants P41EB0135898, U01EB026412, R01CA197254, R01CA172845, R01NS102156 and the UCSF NICO project. The authors would additionally like to thank Romelyn Delos Santos, Kimberly Okamoto, Mary McPolin, and Hope Williams for their help with volunteer studies.

References

[1] J.H. Ardenkjaer-Larsen, On the present and future of dissolution-DNP, J. Magn. Reson. (2016), https://doi.org/10.1016/j.jmr.2016.01.015.
[2] J.H. Ardenkjaer-Larsen, B. Fridlund, A. Gram, et al., Increase in signal-to-noise ratio of > 10,000 times in liquid-state NMR, Proc. Natl. Acad. Sci. 100 (18) (2003) 10158–10163.
[3] S.J. Nelson, J. Kurhanewicz, D.B. Vigneron, et al., Metabolic imaging of patients with prostate cancer using hyperpolarized [1-13C] pyruvate, Sci Transl Med. (2013;5(198):) 198ra108, https://doi.org/10.1126/scitranslmed.3006070.
[4] Ilwoo Park, Peder E.Z. Larson, Jeremy W. Gordon, Lucas Carvajal, Hsin-Yu Chen, Robert Bok, Mark Van Criekinge, Marcus Ferrone, James B. Slater, Duan Xu, John Kurhanewicz, Daniel B. Vigneron, Susan Chang, Sarah J. Nelson, Development of methods and feasibility of using hyperpolarized carbon-13 imaging data for evaluating brain metabolism in patient studies: hyperpolarized Carbon-13 metabolic imaging of patients with brain tumors, Magn. Reson. Med 80 (3) (2018) 864–873, https://doi.org/10.1002/mrm.v80.310.1002/mrm.27077.
[5] K. Golman, R.i. Zandt, M. Lerche, R. Pehrson, J.H. Ardenkjaer-Larsen, Metabolic imaging by hyperpolarized 13C magnetic resonance imaging for in vivo tumor diagnosis, Cancer Res. 66 (22) (2006) 10855–10860, https://doi.org/10.1158/0008-5472.CAN-06-2564.
[6] H.Y. Chen, P.E.Z. Larson, R.A. Bok, et al., Assessing prostate cancer aggressiveness with hyperpolarized dual-agent 3D dynamic imaging of metabolism and perfusion, Cancer Res. 7 (2017) 3207–3217, https://doi.org/10.1158/0008-5472.CAN-16-2083.
[7] R. Aggarwal, D.B. Vigneron, J. Kurhanewicz, Hyperpolarized 1-[13C]-pyruvate magnetic resonance imaging detects an early metabolic response to androgen ablation therapy in prostate cancer, Eur. Urol. 72 (6) (2017) 1028–1029, https://doi.org/10.1016/j.eururo.2017.07.022.
[8] C.H. Cunningham, J.Y.C. Lau, A.P. Chen, et al., Hyperpolarized 13C metabolic MRI of the human heart, Circ. Res. (2016:) 1177–1183, https://doi.org/10.1161/CIRCRESAHA.116.309769.
[9] M.A. Schroeder, H.J. Atherton, M.S. Dodd, et al., The cycling of acetyl-coenzyme A through acetylcarnitine buffers cardiac substrate supply: a hyperpolarized 13C magnetic resonance study, Circ. Cardiovasc. Imaging 5 (2) (2012) 201–209.
[10] M.A. Schroeder, H.J. Atherton, D.R. Ball, et al., Real-time assessment of Krebs cycle metabolism using hyperpolarized 13C magnetic resonance spectroscopy, FASEB J. 23 (8) (2009) 2529–2538.
[11] M.J. Albers, R. Bok, A.P. Chen, et al., Hyperpolarized 13C lactate, pyruvate, and alanine: noninvasive biomarkers for prostate cancer detection and grading, Cancer Res. 68 (20) (2008) 8607–8615.
[12] K.M. Brindle, S.E. Bohndiek, F.A. Gallagher, et al., Tumor imaging using hyperpolarized 13C magnetic resonance spectroscopy, Magn. Reson. Med. 66 (2) (2011) 505–519.
[13] N.M. Anderson, P. Mucka, J.G. Kern, H. Feng, The emerging role and targetability of the TCA cycle in cancer metabolism, Protein Cell. 9 (2) (2018) 216–237, https://doi.org/10.1007/s13238-017-0451-1.
[14] J.L. Izquierdo-Garcia, P. Viswanath, P. Eriksson, et al., IDH1 mutation induces reprogramming of pyruvate metabolism, Cancer Res. 75 (15) (2015) 2999–3009, https://doi.org/10.1158/0008-5472.CAN-15-0840.
[15] M. Marjańska, A.A. Shestov, D.K. Deelchand, E. Kittelson, P.G. Henry, Brain metabolism under different anesthetic conditions using hyperpolarized [1-13 C]pyruvate and [2-13 C]pyruvate, NMR Biomed. 31 (12) (2018), https://doi.org/10.1002/nbm.4012 e4012.
[16] P.A. Bottomley, J.R. Griffiths, et al., Handbook of magnetic resonance spectroscopy in vivo: MRS theory, practice and applications, John Wiley & Sons, 2016.
[17] J.M. Park, S. Josan, T. Grafendorfer, et al., Measuring mitochondrial metabolism in rat brain in vivo using MR Spectroscopy of hyperpolarized [2-^{13}C]pyruvate, NMR Biomed. 26 (10) (2013) 1197–1203, https://doi.org/10.1002/nbm.2935.
[18] A.W. Autry, J.W. Gordon, L. Carvajal, et al., Comparison between 8- and 32-channel phased-array receive coils for in vivo hyperpolarized 13C imaging of the human brain, Magn. Reson. Med. 82 (2019) 833–841, https://doi.org/10.1002/mrm.27743.
[19] M. Vareth, J.M. Lupo, P.E.Z. Larson, et al., A comparison of coil combination strategies in 3D multi-channel MRSI reconstruction for patients with brain tumors, NMR Biomed. 31 (2018), https://doi.org/10.1002/nbm.3929 e3929.
[20] P.E.Z. Larson, H.Y. Chen, J.W. Gordon, et al., Investigation of analysis methods for hyperpolarized 13C-pyruvate metabolic MRI in prostate cancer patients, NMR Biomed. 31 (2018), https://doi.org/10.1002/nbm.3997 e3997.
[21] S. Majumder, C.M. DeMott, D.S. Burz, A. Shekhtman, Using singular value decomposition to characterize protein-protein interactions by in-cell NMR spectroscopy, ChemBioChem. 15 (7) (2014) 929–933, https://doi.org/10.1002/cbic.201400030.
[22] P. Hagmann, L. Cammoun, X. Gigandet, S. Gerhard, et al., MR connectomics: principles and challenges, J. Neurosci. Methods 194 (1) (2010) 34–45, https://doi.org/10.1016/j.jneumeth.2010.01.014.
[23] I. Hotz, T. Schultz, Visualization and processing of higher order descriptors for multi-valued data, first ed., Springer Publishing Company, Incorporated, 2015.
[24] J. Brender, S. Kishimoto, H. Merkle, et al., Dynamic Imaging of Glucose and Lactate Metabolism by ^{13}C-MRS without Hyperpolarization, Sci. Rep. 9 (1) (2019) 3410, https://doi.org/10.1038/s41598-019-38981-1.